In situ Al$_3$Ti and Al$_2$O$_3$ nanoparticles reinforced Al composites produced by friction stir processing in an Al-TiO$_2$ system

Q. Zhang, B.L. Xiao, Q.Z. Wang, Z.Y. Ma *

Shenyang National Laboratory for Materials Science, Institute of Metal Research, Chinese Academy of Sciences, 72 Wenhua Road, Shenyang 110016, China

ARTICLE INFO

ABSTRACT

Al and TiO$_2$ powders were selected to fabricate in situ Al composites via multiple pass friction stir processing (FSP) based on the thermodynamic analysis. The microstructural investigations indicated FSP would induce reaction between Al and TiO$_2$. Al$_3$Ti and Al$_2$O$_3$ particles were formed after 4 pass FSP with 100% overlapping. The in situ particles were about 80 nm in size at various FSP conditions, and ultrafine matrix grains 602 nm in size were obtained when water cooling was applied during FSP. Tensile tests indicated that the in situ nanocomposites exhibited pronounced work hardening behavior and a good combination of strength and ductility.

1. Introduction

Friction stir processing (FSP), a development based on friction stir welding (FSW), is a solid state processing technique for microstructural modification [1] and has been successfully applied to producing in situ intermetallics-reinforced aluminum matrix composites from elemental powder mixtures of Al-Cu and Al-Ti [2]. However, exothermic reactions cannot sufficiently proceed even after four pass FSP with 100% overlapping is applied [2].

The heat release of the Al-Metal oxide (MeO) reaction is much higher than that of the Al-transition metal [3]. Thus a higher temperature and a more enhanced reaction are expected in the Al-MeO system. Recently, Chen et al. [4] successfully fabricated in situ (Al$_{11}$Ce$_3$ + Al$_2$O$_3$)/Al composites in an Al-CeO$_2$ system by FSP. However, because the thermite reaction between Al and CeO$_2$ was severe, a large amount of heat was released. Thus, FSP had to be conducted at a low tool rotation rate of 500 rpm in order to obtain defect-free samples. Even at a lower FSP heat input, the main reinforcement Al$_{11}$Ce$_3$ was larger than 1 μm in size. In this case, the resultant composites exhibited low ductility (~3%).

In this study, Al and TiO$_2$ were selected as the raw materials based on the following considerations. First, the heat release of the reaction between Al and TiO$_2$ ($\Delta H = -146.4$ KJ/mol) is much lower than the one between Al and CeO$_2$ ($\Delta H = -574$KJ/mol) [3]. Second, the solid reaction between Al and TiO$_2$ always involves several steps [5], so the heat release would be relatively gentle. Therefore, the growth of Al$_3$Ti

would be effectively controlled during the fabrication. The aim of the present study is (1) to fabricate the in situ composites with nanosized particles in the Al-TiO$_2$ system via FSP and (2) to understand the tensile behavior of the in situ nanocomposites.

2. Experimental

Commercial pure Al powder (99.9% purity, 13 μm) and TiO$_2$ powder (Rutile, 99% purity, 1.2 μm) were used. The volume fraction of reinforcements (Al$_3$Ti + Al$_2$O$_3$) would be 25%, assuming that the reaction goes to completion to form Al$_3$Ti and Al$_2$O$_3$. The as-mixed powders were hot pressed into billets and then hot forged at 723 K into disc plates 10 mm in thickness. The plates were subjected to 4 pass FSP with 100% overlapping in air (defined as FSP-air). Furthermore, some FSP-air samples were subjected to additional 2 pass FSP with 100% overlapping in flowing water (defined as FSP-water). The samples were first fixed in room temperature water and additional rapid cooling with flowing water was used during FSP with the thickness of the water layer in the flume being about 50 mm. The FSP parameters used in this study are shown in Table 1. A cermet tool with a concave shoulder 20 mm in diameter and a threaded cylindrical pin 6 mm in diameter and 5 mm in length was used.

Microstructural investigations were performed on the transverse cross-section of the stir zone (SZ) by X-ray diffraction (XRD) and transmission electron microscopy (TEM) equipped with energy dispersive spectrometer (EDS). Dogbone-shaped tensile specimens (5.0 mm gage length, 1.4 mm gage width, and 1.0 mm gage thickness) were electrodischarge machined from the SZ transverse to the FSP direction. Tensile tests were conducted on an INSTRON 5848 micro-tester at a strain rate of 1×10^{-3} s^{-1}.

* Corresponding author. Tel./fax: +86 24 83978908.
E-mail address: zyma@imr.ac.cn (Z.Y. Ma).

Table 1
The FSP parameters used in this study.

	Rotation rate, rpm	Travel speed, mm/min	FSP pass
FSP-air	1000	25	4
FSP-water	1000	25/50	6[a]

[a] The first four FSP passes were carried out at a travel speed of 25 mm/min and the final two FSP passes were carried out at 50 mm/min in flowing water.

3. Results and discussion

Fig. 1 shows the XRD patterns of various samples. In the forged sample, strong diffraction peaks of Al and TiO_2 and weak peaks of Al_3Ti were identified, indicating that a weak reaction between Al and TiO_2 took place during the hot pressing and forging. In the FSP-air sample, the TiO_2 peaks disappeared, and some strong peaks of Al_3Ti and α-Al_2O_3 appeared. In addition, some weak TiO peaks were revealed. The identified phases in the FSP-water sample are the same as those in the FSP-air sample. The XRD results indicate that four pass FSP under the investigated parameters induced the reaction between Al and TiO_2, forming Al_3Ti, α-Al_2O_3, and a small quantity of TiO.

Feng and Froyen [5] reported that the reactive products between Al and TiO_2 were TiO and γ-Al_2O_3 before the melting of Al, and Al_3Ti and α-Al_2O_3 after the melting of Al. Although the maximum temperature in the SZ during FSP could not have exceeded the melting temperature of Al [1], the main products of the Al-TiO_2 reaction during FSP were Al_3Ti and α-Al_2O_3 rather than γ-Al_2O_3 and TiO.

Barlow et al. [6] and Ying et al. [7] found that mechanical milling facilitated the formation of Al_3Ti and α-Al_2O_3 in the Al-TiO_2 system in the solid state due to the effect of mechanical activation. However, Al_3Ti and α-Al_2O_3 need an incubation time to form after mechanical milling, and the incubation time of α-Al_2O_3 is much longer than that of Al_3Ti. It was reported that in the temperature range of 500 to 600°C, the incubation time of α-Al_2O_3 might be as long as several hours [6,7]. In this study, Al_3Ti and α-Al_2O_3 formed within only a few seconds during FSP. The accelerated forming of Al_3Ti and α-Al_2O_3 is attributed to the following factors. First, severe plastic deformation of FSP broke up the oxide film on the Al particles, which caused intimate contact between Al and TiO_2, and then reduced the diffusion distance of elements. Second, the high density of dislocations produced by severe plastic deformation during FSP not only provided the nucleation sites of Al_3Ti and α-Al_2O_3 but also assisted in growth of an embryo beyond the critical size by providing a diffusion pipe [8,9].

Fig. 2 shows the TEM images of the FSP samples. A high density of particles about 80 nm in average size was randomly distributed both within the grain interiors and at the grain boundaries for both FSP
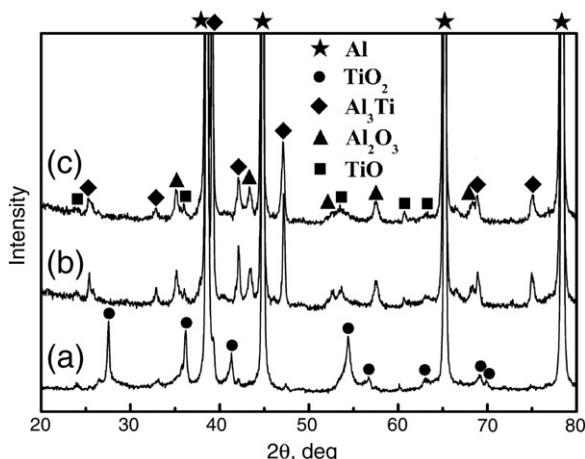

Fig. 1. XRD patterns of (a) forged sample, (b) FSP-air sample, (c) FSP-water sample.

samples. The volume fraction of the nanoparticles with the size below 100 nm is estimated to be 7.4% in both FSP samples from at least 10 TEM images. Selected area diffraction analyses indicated that these particles were Al_3Ti and α-Al_2O_3 (Fig. 2(c)). The formation of nanosized particles is attributed to following factors. First, as mentioned above, the heat release from the reaction of Al and TiO_2 is relatively gentle. Second, the coarsening rates of Al_3Ti and Al_2O_3 are very low at 500~600°C [4,6]. Third, the duration of FSP is very short. Thus, nucleated particles exhibited only limited growth, thereby retaining a nanoscale under various FSP parameters.

The grain sizes in the FSP-air and FSP-water samples were determined, by averaging the sizes of about 100 grains, to be 1285 and 602 nm, respectively (Fig. 2(a)-(b)). This indicates that rapid cooling after FSP effectively inhibited the growth of the recrystallized grains. Similar results were also reported in the Al-Mg-Sc alloy [10]. In addition, a low density of dislocations was observed in the FSP samples. Fig. 2(d) shows the typical dislocation morphology of the FSP-water sample. Most of the dislocations were pinned by nanosized particles. Furthermore, some particles agglomerations with sizes of 200~600 nm were found in the FSP samples (black arrow in Fig. 2(a)-(b)). EDS analyses showed that these agglomerations contained Al, Ti and O. These particles might be intermediate products of the Al-TiO_2 reaction, such as TiO, various polymorphs Al_2O_3, etc [6,7]. Further investigation is required to determine the detailed structures of these agglomerations.

Fig. 3(a) and (b) show the engineering stress-strain curves of the FSP samples and the variation of normalized work-hardening rate (Θ) with the true strain. Θ is defined as:

$$\Theta = \frac{1}{\sigma} \left(\frac{\partial \sigma}{\partial \varepsilon} \right)_{\dot{\varepsilon}} \tag{1}$$

where σ and ε are the true stress and true strain, respectively. A pronounced strain hardening was observed in the FSP samples even when the grain size was reduced to 602 nm, compared with ultrafine-grained pure Al (750 nm) produced via equal channel angular pressing coupled with annealing treatment [11]. The yield strength (YS), ultimate tensile strength (UTS) and uniform elongation of the FSP-air sample are 210 MPa, 286 MPa and 11.5%, respectively. By comparison, the FSP-water sample exhibited much higher YS and UTS due to finer grain size, whereas the uniform elongation decreased to 6.8%, which was still above the critical ductility (5%) required for many structural applications.

Compared with ex situ nanocomposites with similar matrix grain sizes [11,12], the in situ composites in this study exhibited higher strength due to a higher particle volume fraction. Generally, a higher reinforcement volume fraction would result in lower ductility for particle reinforced composites [13]. However, the in situ composites in this study exhibited comparable elongations with the ex situ composites. This is attributed to the following factors.

First, the dislocation density in the samples fabricated by FSP is remarkably lower than that in samples fabricated by other methods [10,14]. Thus the FSP samples would have more sites for nucleating and accommodating dislocations, thereby enhancing their work hardening capacity [15]. Second, as shown in Fig. 2(d), a small quantity of dislocations was maintained after FSP due to the pinning effect of the nanosized particles. These initial dislocations would be difficult to drive and annihilate during tensile testing [16,17]. Therefore, a higher strain hardening capacity was obtained, leading to a larger strain and higher strength [10,15,17].

4. Conclusions

In summary, FSP induced the reaction between Al and TiO_2, producing in situ Al_3Ti and Al_2O_3 particles about 80 nm in size. Ultrafine matrix grains 602 nm in size were obtained by FSP with water cooling.
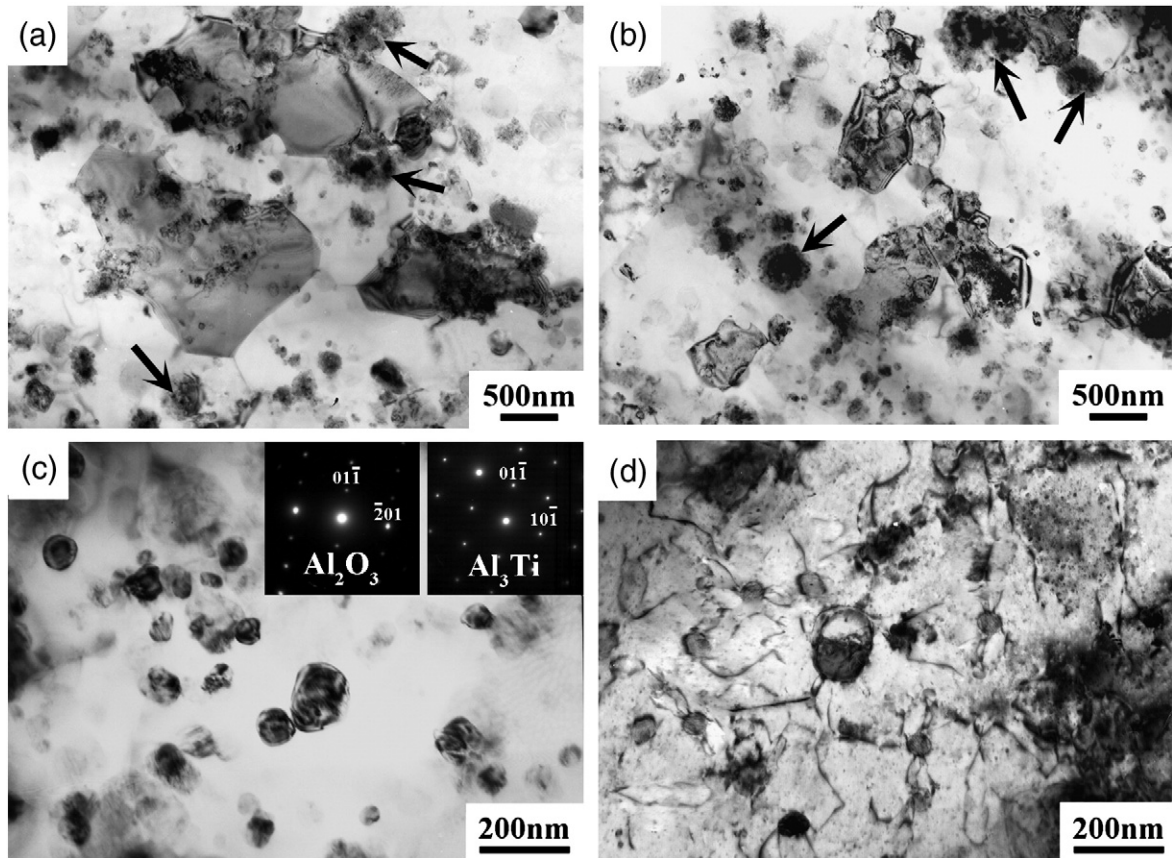
Fig. 2. TEM images showing grains and second phase particles: (a) FSP-air sample; (b), (c) and (d) FSP-water sample.
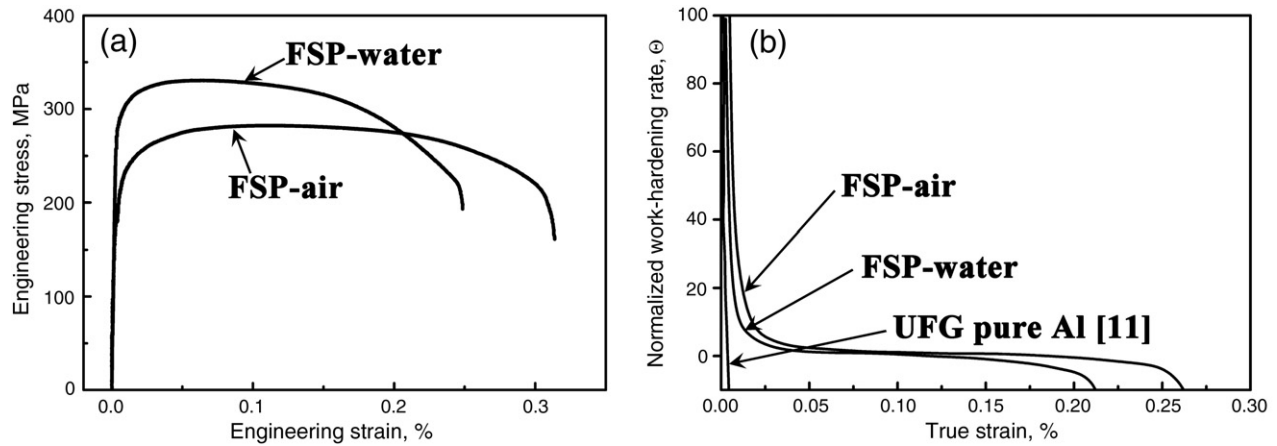

Fig. 3. (a) Engineering stress-strain curves and (b) the variation of normalized work-hardening rate (Θ) with the true strain of the FSP samples.

The in situ nanocomposites exhibited a good combination of strength and ductility compared with the ex situ composites.

Acknowledgements

References

[1] Mishra RS, Ma ZY. Mater Sci Eng R 2005;50:1–78.
[2] Hsu CJ, Kao PW, Ho NJ. Mater Lett 2007;61:1315–8.
[3] Barin I. Thermochemical Date of Pure Substances. third ed. Stuttgart: VCH Verlagsgesellschaft; 1995.
[4] Chen CF, Kao PW, Chang LW, Ho NJ. Metall Mater Trans A 2010;41:513–22.
[5] Feng CF, Froyen L. Composites Part A 2000;31:385–90.
[6] Barlow IC, Jones H, Rainforth WM. Acta Mater 2001;49:1209–24.
[7] Ying DY, Zhang DL, Newby M. Metall Mater Trans A 2004;35:2115–25.
[8] Shu JQ, Nelson TW, Mishra R, Mahoney M. Acta Mater 2003;51:713–29.
[9] Porter DA, Easterling KE. Phase Transformation in Metal and Alloys. second ed. London: Chapman & Hall; 1992.
[10] Liu FC, Ma ZY, Chen LQ. Scripta Mater 2009;60:968–71.
[11] Hu CM, Lai CM, Du XH, Ho NJ, Huang JC. Scripta Mater 2008;59:1163–6.
[12] Kang YC, Chan SI. Mater Chem Phys 2004;85:438–43.
[13] Lloyd DJ. Int Mater Rev 1994;39:1–23.
[14] Jata KV, Semiatin SL. Scripta Mater 2000;43:743–9.
[15] Cheng S, Zhao YH, Zhu YT, Ma E. Acta Mater 2007;55:5822–32.
[16] Humphreys FJ, Hatherly M. Recrystallization and Related Annealing Phenomena. second ed. Oxford: Elsevier Ltd; 2004.
[17] Ma E. JOM 2006;4:49–53.